Journal of Bacteriology

The Major Autolysin Acm2 from Lactobacillus plantarum Undergoes Cytoplasmic O-Glycosylation

Lasse Fredriksen, Geir Mathiesen, Anders Moen, Peter A. Bron, Michiel Kleerebezem, Vincent G. H. Eijsink and Wolfgang Egge-Jacobsen

J. Bacteriol. **2012, 194(2):325. DOI: 10.1128/JB.06314-11. Published Ahead of Print 11 November 2011.**

JB
Journals.ASM.org

The Major Autolysin Acm2 from *Lactobacillus plantarum* Undergoes Cytoplasmic O-Glycosylation

Lasse Fredriksen,[a] Geir Mathiesen,[a] Anders Moen,[b] Peter A. Bron,[c,d] Michiel Kleerebezem,[c,d,e] Vincent G. H. Eijsink,[a] and Wolfgang Egge-Jacobsen[b]

Department of Chemistry, Biotechnology and Food Science, Norwegian University of Life Sciences, Aas, Norway[a]; Department of Molecular Biosciences, Glyconor Mass Spectrometry, University of Oslo, Oslo, Norway[b]; NIZO Food Research, Ede, The Netherlands[c]; TI Food & Nutrition, Wageningen, The Netherlands[d]; and Host-Microbe Interactomics Group, Wageningen University and Research Centre, Wageningen, The Netherlands[e]

The major autolysin Acm2 from the probiotic strain *Lactobacillus plantarum* WCFS1 contains high proportions of alanine, serine, and threonine in its N-terminal so-called AST domain. It has been suggested that this extracellular protein might be glycosylated, but this has not been experimentally verified. We used high-resolution liquid chromatography-tandem mass spectrometry (LC-MS/MS) to study the possible occurrence of glycans on peptides generated from lactobacillary surface proteins by protease treatment. This approach yielded five glycopeptides in various glycoforms, all derived from the AST domain of Acm2. All five glycopeptides contained the hydroxy-amino acids serine and threonine, suggesting that Acm2 is O-glycosylated. By using lectin blotting with succinylated wheat germ agglutinin, and by comparing the wild-type strain with an Acm2-negative derivative (NZ3557), we found that the attached *N*-acetylhexosamines are most likely *N*-acetylglucosamines (GlcNAc). NZ3557 was further used as a genetic background to express an Acm2 variant lacking its secretion signal, resulting in intracellular expression of Acm2. We show that this intracellular version of Acm2 is also glycosylated, indicating that the GlcNAc modification is an intracellular process.

Glycosylation is involved in a variety of biological processes and is one of the most common protein modifications. In protein glycosylation, glycan moieties are generally attached to serine or threonine (O-linked glycosylation) or to asparagine (N-linked glycosylation) residues. In eukaryotes, a vast number of glycoproteins have been identified and characterized, whereas bacterial protein glycosylation is still considered to be relatively rare (30). Bacterial glycoproteins described so far are mainly abundant polymeric surface proteins such as flagellins, pilins, and S-layer proteins (2, 23, 36), as well as virulence factors of pathogens (11, 17, 45). A general O-glycosylation system in *Neisseria gonorrhoeae* has been described (48), and numerous O-glycosylated proteins have also been discovered in the Gram-negative major gut symbiont *Bacteroides fragilis* (12). In Gram-positive pathogens, such as streptococci and staphylococci, several serine-rich fimbria-like adhesins undergo glycosylation (4, 33, 41). In lactobacilli, the only glycoproteins characterized to date are S-layer proteins, in addition to a peptide bacteriocin (27, 29, 44).

Lactobacillus plantarum is one of the most studied *Lactobacillus* species and is considered a versatile bacterium capable of adapting to a variety of environmental niches such as vegetable, meat, and dairy substrates (42). In addition, *L. plantarum* is among the predominant *Lactobacillus* species found in the human gastrointestinal tract (1), and some strains are regarded as probiotic (10, 28). *L. plantarum* WCFS1 is a single-colony isolate of the human pharyngeal strain NCIMB8826 and is recognized as a model probiotic bacterium (19, 47). This organism has the largest *Lactobacillus* genome sequenced to date (3.3 MB). This genome encodes 3,018 proteins, of which 222 are annotated as encoding secretome proteins (6) (see http://www.cmbi.ru.nl/lab_secretome for detailed information on the predicted secretome).

Secreted proteins are likely to play major roles in the interaction between the bacterium and its environment (34) and are thus important for bacterial behavior. Among the extracellular enzymes in *L. plantarum* is the major autolysin Acm2 (32).This enzyme is an *N*-acetylglucosaminidase responsible for cleavage of the β-1-4 bond between *N*-acetylglucosamine (GlcNAc) and *N*-acetyl muramic acid (MurNAc) of peptidoglycan in the cell wall (5). It has been demonstrated that Acm2 is functionally similar to AcmA from *Lactococcus lactis*, and inactivation of its corresponding gene results in incomplete cell separation (32). Acm2 contains five C-terminal SH3 repeats, and previous studies have shown that these are most likely involved in cell wall binding (24, 50). The N-terminal domain of Acm2 is rich in alanine, serine, and threonine and is referred to as the AST domain. The functional role of AST domains is unknown, but their importance is suggested by the fact that similar domains occur in 11 of 16 *L. plantarum* peptidoglycan hydrolases. While glycosylation of non-surface-layer proteins in lactobacilli has not yet been described, it has been hypothesized that the AST domains in proteins such as Acm2 could be glycosylated (20).

The advent of high-resolution mass spectrometry-based methods for protein identification has opened up new avenues for the detection of posttranslational modifications (22). Here, we used these techniques to search for the occurrence of glycosylated proteins in the secretome of *L. plantarum*. This led to the discovery that the AST domain of Acm2 is glycosylated with 15 HexNAc

Received 3 October 2011 **Accepted** 31 October 2011
Published ahead of print 11 November 2011
Address correspondence to Vincent G. H. Eijsink, vincent.eijsink@umb.no, or Wolfgang Egge-Jacobsen, w.m.egge-jaobsen@imbv.uio.no.

doi:10.1128/JB.06314-11
The authors have paid a fee to allow immediate free access to this article.

TABLE 1 Strains and plasmids used in this study

Strain or plasmid	Relevant characteristic(s)	Reference
Strains		
L. plantarum		
WCFS1	Host strain	19
NZ3557	Cm^r; WCFS1 derivative; *acm2*::*cat*	This work
E. coli Top10	Host strain	Invitrogen
Plasmids		
p2588sAmyA	Em^r; pSip401 derivative (43), containing the inducible P_{sppA} promoter translationally fused to the Lp_2588 signal peptide followed by AmyA	26
pAcm2	Em^r; pLp_2588sAmyA derivative with the *acm2* gene translationally fused to the P_{sppA} promoter, encoding secreted Acm2	This work
pCytAcm2	Em^r; pAcm2 derivative with a trunctated *acm2* gene translationally fused to the P_{sppA} promoter; encoding cytoplasmic Acm2	This work
pNZ5319H9	Cm^r Em^r; pNZ5319 derivative (21) with an H9 DNA tag[a]	I. van Swam
pNZ3557	Cm^r Em^r; pNZ5319H9 derivative containing homologous regions up- and downstream of the *acm2* gene	This work

[a] The H9 DNA tag (CTTTCAATCTTTGTTTCTATCTTACTTTCTTTCTTGCATACT) is located downstream of the *lox71* site. This tag was not specifically used in this study.

moieties, which are most likely added prior to export of the protein.

MATERIALS AND METHODS

Bacterial strains, cultivation, and DNA manipulations. The bacterial strains and plasmids used in this study are listed in Table 1. *Escherichia coli* TOP10 cells (Invitrogen, Carlsbad, CA) were aerobically grown in BHI broth (Oxoid Ltd., Basingstoke, United Kingdom) or TY broth (18) at 37°C with shaking. *Lactobacillus plantarum* and its derivative NZ3557 (19) were grown in MRS (Oxoid) without aeration at 37°C. Solid media were prepared by adding 1.5% (wt/vol) agar to the broth. The antibiotic concentrations used for positive clone selection were 5 μg/ml and 200 μg/ml erythromycin for *L. plantarum* and *E. coli*, respectively.

All PCR amplifications were performed with hot-start KOD polymerase (Toyobo, Osaka, Japan). PCR fragments were purified using the Nucleo-Spin extract II kit (Macherey-Nagel GmbH & Co., Düren, Germany). Plasmid DNA was purified using the NucleoSpin plasmid kit (Macherey-Nagel GmbH & Co) or the Jetstar Midi-Prep plasmid purification system (Genomed GmbH, Germany). *L. plantarum* was transformed by electroporation according to a previously described method (16). The DNA sequences of all PCR-generated amplicons cloned into plasmids were confirmed by sequence analyses.

Construction of a Δ*acm2* knockout mutant. The *acm2* gene was deleted using the Cre-*lox* system as previously described (21), with some modifications. A variant of pNZ5319 designated pNZ5319TAG-H9 (P. A. Bron et al., unpublished data) was used as mutagenesis vector. By using this vector, a unique 42-bp DNA tag is introduced in the mutant, allowing mutant-specific tracking and identification in competitive experiments (not relevant for the experiments reported here). Genomic DNA from *L. plantarum* WCFS1 was isolated as described before (16). The flanking regions upstream and downstream of the *acm2* gene, about 1,000 bp each, were amplified using the primer pairs acm2LF-F/acm2LF-R and acm2RF-F/acm2EF-R, respectively (Table 2). In addition, the *lox-cat-lox* fragment of pNZ5319H9 was amplified using primers is128-lox66-F2 and is129-lox71-R2. The resulting amplicons were used as templates in a SOE (splicing by overlapping extension) PCR (14), where complementarity in the 5′ regions of the primers resulted in linkage of the *acm2*-flanking regions to both sides of the *lox-cat-lox* fragment. The final SOE PCR product was ligated into Swa1-Ecl136II-digested pNZ5319H9, yielding the plasmid pNZ3557. The plasmid, which does not replicate in *L. plantarum*, was transformed into *E. coli*, purified, and electroporated into *L. plantarum*. Chloramphenicol-resistant transformants were selected and subsequently replica plated to check for erythromycin sensitivity. A correct pNZ3557 integrant in the *acm2* locus was confirmed by PCR analysis using primers acm2HF and acm2HR (Table 2), which anneal to adjacent genomic regions. A single *acm2* disruption mutant was isolated and used in subsequent studies.

Construction of Acm2 plasmids. All Acm2 expression vectors used in this study (Table 1) are derivatives of pSIP401, a 5.67-kb vector designed for inducible gene expression in lactobacilli (43) and further developed

TABLE 2 Primers used in this study

Primer	Sequence[a]
acm2F	GATTCCAGTTTCAGCAGGGC
acm2LF-F	GGTATACCTTCTTATTGTATTGGC
acm2LF-R	**CATTAGTCTCGGACATTCTGCTCCCG**CATTCCAATTTTCAATTTTAAAATCCCC
acm2RF-F	**CCGATCGCTACGAGAAGACGCACTA**GGCTAGGCATATTAGTTGTTCCG
acm2RF-R	AGGCCGTAAATTCGTGACCC
acm2HF	GATTCCAGTTTCAGCAGGGC
Acm2HR	GTGATATTCTGATATTCTGGCGC
IFacm2cytF	GGAGTATGATTCATATGGACAGTACAGGACCGCAAAGCC
IFacm2F	GGAGTATGATTCATATGAAAATTGGAATGACAAAAAAAGTAGTAAC
IFacm2R	CCGGGGTACCGAATTCCTAGCCTTCAAGCTTAGCAACATAGT
is128-lox66-F2	CGGGAGCAGAATGTCCGAGACTAATG
is129-lox71-R2	TAGTGCGTCTTCTCGTAGCGATCGG

[a] Boldface indicates parts of the primers that are complementary to the is128-lox66-F2 and is129-lox71-R2 primers; underlining indicates 15-bp extensions that are complementary to the ends of the NdeI-EcoRI digested p2588sAmyA vector, necessary for in-fusion cloning (In-Fusion HD cloning kit).

for protein secretion and anchoring (13, 26). These vectors were constructed in order to complement the *acm2* mutant with either native Acm2 or an N-terminally truncated version of Acm2 for cytoplasmic expression. The *acm2* ORF was amplified from the *L. plantarum* genome with primers IFacm2F and IFacm2R (Table 2). The PCR product was cloned directly into NdeI-EcoRI-digested p2588sAmyA (a pSIP401 derivative) (Table 1) using the In-Fusion HD cloning kit (Clontech Laboratories, Mountain View, CA), following the manufacturer's instructions. This yielded the plasmid pAcm2 (Table 1), which allows inducible expression of Acm2 with its native signal peptide. A plasmid encoding intracellular Acm2 (pCytAcm2, lacking 111 N-terminal amino acids) was constructed using the same cloning strategy as for pAcm2, except that IFacm2CytF was used as forward primer.

Trypsin digestion of agar medium-grown cells. Bacteria from a −80°C glycerol stock were streaked on MRS plates and incubated at 37°C for ~18 h. Subsequently, 3 ml of phosphate-buffered saline (PBS) was added, and the plates were swirled slowly on a shaker for 10 min to suspend the cells. The cell suspension was transferred to Eppendorf tubes and centrifuged at 500 × *g* for 3 min. The pellet was washed once in PBS and recentrifuged. The cells were then washed in trypsin buffer (50 mM ammonium bicarbonate) and recentrifuged. Proteomics grade trypsin (500 ng; Sigma) solubilized in 200 μl trypsin buffer was added and the resulting cell suspension was incubated in a 37°C shaker at 700 rpm for 45 to 90 min. The samples were centrifuged, and tryptic peptides were collected by ultrafiltration of the supernatant at 13,000 × *g* through a 10-kDa Pall Nanosep centrifugal device (Sigma). The filtrate was transferred to vials, and the peptide mixtures were subsequently analyzed by liquid chromatography-tandem mass spectrometry (LC-MS/MS).

Isolation of intracellular and surface proteins. Fresh overnight cultures of *L. plantarum* WCFS1 and its derivatives were diluted in fresh MRS and induced at an optical density at 600 nm (OD_{600}) of 0.1 by adding 25 μg/ml peptide pheromone, as previously described (25). After 6 h of growth at 37°C, the cells were harvested by centrifugation at 3,000 × *g* for 10 min at 4°C. All the following steps were performed at 4°C. To remove medium components, the cells were rapidly washed with PBS (137 mM NaCl, 2.7 mM KCl, 4.3 mM Na_2HPO_4, 1.47 mM KH_2PO_4 [pH 7.4]) and recentrifuged. Surface proteins were extracted by incubation with 1 ml cold PBS for 30 min under gentle agitation. The cell suspension was subsequently centrifuged at 5,000 × *g* for 10 min. The resulting supernatant was transferred to a clean Eppendorf tube, and the proteins were precipitated by addition of 16% (final concentration) trichloroacetic acid (TCA) followed by incubation on ice for 20 min. After centrifugation at 16,000 × *g* for 15 min, the precipitated proteins were washed with 200 μl acetone and collected by recentrifugation. The protein pellets were dried in a Speedvac and solubilized directly in NuPAGE loading buffer and reducing agent (both from Invitrogen). The NuPAGE buffer volumes were adjusted according to the OD_{600} of the original culture to ensure that all samples used for subsequent sodium dodecyl sulfate-polyacrylamide gel electrophoresis (SDS-PAGE) represented similar amounts of cells. The cell pellets were washed once with PBS, resuspended in 1 ml PBS, and disrupted with glass beads (≤106 μM; Sigma, St. Louis, MO), after which cell debris was removed by centrifugation at 16,000 × *g* for 10 min. The resulting cell extracts were stored at −20°C until use. Sample sizes in subsequent SDS-PAGE were adjusted according to the OD_{600} of the original culture to ensure that all samples represented similar amounts of cells.

SDS-PAGE. Samples containing NuPage loading buffer and reducing agent were mixed by using a Vortex and boiled for 10 min prior to SDS-PAGE. Proteins were separated under denaturing conditions on 10% NuPAGE Novex bis-Tris gels (Invitrogen) and stained with Coomassie blue R-250.

In-gel protein trypsinization. In-gel trypsinization of proteins separated by SDS-PAGE was performed according to the method described by Shevchenko et al. (40). Solubilized tryptic peptides were analyzed by liquid chromatography combined with mass spectrometry (LC-MS).

Lectin blotting. Surface proteins separated on SDS-PAGE were transferred to a nitrocellulose membrane (iBlot system; Invitrogen). The membrane was incubated with 25 μg biotinylated succinylated wheat germ agglutinin (sWGA; Vector Labs, Burlingame, CA) and subsequently with 20 ng streptavidin–poly-HRP (streptavidin conjugated to horseradish peroxidase polymers; ImmunoTools GmbH, Friesoythe, Germany) using the SNAP i.d. system (Millipore, Billerica, MA), according to the protocol provided by the manufacturer. Proteins interacting with sWGA, which is specific for GlcNAc, were visualized with the SuperSignal West Pico chemiluminescent substrate (Pierce, Rockford, IL). Proteins used as controls, RNase B and bovine serum albumin (BSA), were purchased from New England BioLabs (Ipswich, MA).

LC-MS/MS analysis. Reverse-phase (C_{18}) chromatography of tryptic peptides was carried out using a high-pressure liquid chromatography (HPLC) system consisting of two Agilent 1200 HPLC binary pumps (nano and capillary) with an autosampler, a column heater, and an integrated switching valve. The LC system was coupled via a nanoelectrospray ion source to an LTQ-Orbitrap mass spectrometer (Thermo Fisher Scientific, Bremen, Germany). For the analyses, 4 μl of peptide solution were first injected into a 5- by 0.3-mm extraction column filled with Zorbax 300 SB C_{18} with a particle size of 5 μm (Agilent). After a washing for 7 min with 0.1% (vol/vol) formic acid, 3% (vol/vol) acetonitrile at a flow rate of 4 μl/min, the switching valve was activated, and the peptides were eluted in the back-flush mode from the extraction column onto a 150- by 0.075-mm C_{18} column (3-μm particle size; GlycoproSIL C18-80Å; Glycopromass, Stove, Germany). The mobile phase consisted of acetonitrile and MS-grade water, both containing 0.1% formic acid. Chromatographic separation was achieved using a binary gradient from 5 to 55% of acetonitrile in 60 or 120 min. The nanoflow pump flow rate was 8 μl/min. Mass spectra were acquired in the positive-ion mode applying a data-dependent automatic switch between survey scan and tandem mass spectrum (MS/MS) acquisition. Peptide samples were analyzed either by higher-energy C-trap dissociation (HCD) or by collision-induced dissociation (CID) in the LTQ ion trap by acquiring one Orbitrap survey scan in the mass range of 200 to 2000, followed by HCD and/or CID of the three most intense ions in the Orbitrap. The target value in the LTQ-Orbitrap was 1,000,000 for survey scan at a resolution of 30,000 at *m/z* 400 using lock masses for recalibration to improve the mass accuracy of precursor ions. Fragmentation was performed with a target value of 5,000 ions. The ion selection threshold was 500 counts. Selected sequenced ions were dynamically excluded for 180 s.

MS data analysis. Mass spectrometric data were analyzed using the *L. plantarum* WCFS1 genome sequence and the SEQUEST software package. The mass tolerances for a fragment ion and a parent ion were set to 0.05 Da and 7 ppm, respectively. Methionine oxidation and cysteine carbamidomethylation were selected as a variable and a fixed modification, respectively. A false-discovery rate of 0.01 was set for proteins and peptides with a minimum length of 6 amino acids. MS/MS spectra of putative glycopeptides were manually inspected using Qual Browser version 2.0.7

RESULTS

Identification of Acm2 glycopeptides. Intact *L. plantarum* cells were trypsinized, and the resulting peptides were analyzed by online nano-LC-MS/MS using the Orbitrap XL mass spectrometer in the higher-energy C-trap dissociation (HCD) fragmentation mode. To perform glycoprofiling on tryptic peptides from *L. plantarum*, we took advantage of the formation of the strong diagnostic oxonium ions at *m/z* 204.085 that emerge upon HCD fragmentation of glycopeptides containing *N*-acetylhexosamine (HexNAc) (35). Furthermore, we used losses of 203.079 Da within the higher *m/z* region to identify glycopeptides containing HexNAc. These diagnostic ion signals were used to select specific MS/MS spectra for further subsequent fragmentation analysis. Five different peptides met these criteria, all originating from

A

B

SPase I ↓ CytAcm2 ↓

MKIGMTKKVVTSLLLSTALLPMLSGKADTASANQKPAAATK**GNSAASAASQQVTLSAGSQ**
TETTAAGATDQSVASDGAKTDDQAESTSTTTATTSATSRVTVRAASQAAKA**DSTGPQSQS**
SASEAAKDNAATSATADSTTSAVDQLDKTAK**ASAATSQASHSTTNETAKASAAASQDSHV**
TTDQSSVTVTSEVAKSAASSAAPK**QATEQAVAAK**ISPK**IETAVAADAVQSSAMMAR**STR**A**
MTSQEIFLSQIKAGAISGWNKYQVLPSVTAAQAILESGWGQSQLATQGNNLFGIKGSYQG
QSIYFPTQEWNGSQYITIQDAFRKYPNWSASVEDHGAFLVVNPR**YSNLIGVTDYRRVASLL**
QQDGYATAPTYASSLISIIEYNK**LHEWDQEALSGQASGGNDNNQVQPDQDVTPTSGTHK**
FTK**TTTIHNAPDATSAVVGTYNAGETVNYNGKLTVGNATWLRYQSYSGVSRYVMISQTT**
TNDNNNQATVTPASGSYKFTAKTNIRSAASKT**AQVVGTYNAGETVYYNGKITTGGTTWL**
RYLSYSGAQHYVAMSGDEVGSVAKPDVVATSGSYRFTKTTAIK**SSPATSATTVGSYNAGDT**
VYYNGKVTTNGQTWLRYMSYSGAQHYVQISGESTSTNVDKPQVTPQSGSYR**FTQTTAIK**
NTPAGNAPSVGTYSAGDTVYYNAKVTANGQTWLRYLSYSGAQHYVAISGNAATGNTTSK
PVTNSQGAFR**FVTTTNIR**TAPSTRASVVGEYNPGETVYYNGTVQAEGYTWLRY
LSR**SGATHYVAK**LEG

C

Glycopeptides	No. of HexNAcs
GNSAASAASQQVTLSAGSQTETTAAGATDQSVASDGAK	3,2,1,0
TDDQAESTSTTTATTSATSR	3,2,1,0
ADSTGPQSQSSASEAAK	3,2,1,0
DNAATSATADSTTSAVDQLDK	3,2,1
ASAAASQDSHVTTDQSSVTVTSEVAK	3,2,1,0

FIG 1 Domain structure, identified tryptic fragments, and glycopeptides in Acm2. The peptides were analyzed by MS/MS using the Orbitrap XL mass spectrometer in the HCD fragmentation mode. (A) Modular structure of Acm2. The protein consists of the signal peptide (SP), a (glycosylated) AST domain, an enzymatic domain belonging to glycosyl hydrolase family 73 (GH73), and an SH3 domain with SH3b repeats. (B) Primary amino acid sequence of Acm2. The AST domain is shown in a gray box. The arrows indicate the predicted cleavage site for signal peptidase I (SPase I) and the first amino acid of the truncated, cytoplasmic version of Acm2 (CytAcm2; see the text for more details). A second putative SPase I cleavage site (see the text; AGA ↓ T) is indicated by the line above the sequence. Detected Acm2 peptides are shown in bold, and glycopeptides are underlined. (C) Overview of the HexNAc glycoforms detected for each glycopeptide. All detected glycopeptides were detected in 3 glycoforms, except for DNAATSATADSTTSAVDQLDK, which is the only peptide for which the unglycosylated form was not detected.

Acm2 (Fig. 1). Representative examples of MS/MS spectra are shown in Fig. 2. The fragmentation spectrum obtained for a triply charged ion corresponding to a glycopeptide containing three HexNAcs (Fig. 2A) shows series of y and b ions confirming the sequence of the peptide (peptide fragments that contain the N terminus of the peptide yield b ions, whereas fragments containing the C terminus yield y ions). In addition, and most importantly, the spectrum shows the diagnostic oxonium reporter ion for HexNAc (m/z = 204.085), confirming the glycosylation (see the legend to Fig. 2 for more details). An MS/MS spectrum collected at lower fragmentation energy (Fig. 2B) shows partially and fully deglycosylated full-length fragments of this same precursor ion, as well as the HexNAc oxonium ion (m/z 204.085). The MS analyses did not reveal any oxonium ions for other compounds than single HexNAc glycans (e.g., disaccharide HexNAc-HexNAc with oxonium ion at m/z 407.165), indicating that the glycans attached to Acm2 each consist of a single HexNAc.

A total of 34 unique Acm2 peptides were identified, which corresponds to a sequence coverage of 57.1%. The five identified glycopeptides are all located in the AST domain of Acm2 (Fig. 1B), for which the sequence coverage was 83.2%. Similar experiments using the endopeptidases chymotrypsin or proteinase K instead of trypsin did not yield extra sequence coverage nor detection of additional glycosylation sites (data not shown). As summarized in Fig. 1C, four of the five identified glycopeptides were detected in three glycoforms (singly, doubly, and triply glycosylated with HexNAc) in addition to being detected in an unglycosylated state. All five glycopeptides contained the hydroxy-amino acids serine and threonine, while only two of them contained asparagines. This indicates that the glycosylation of Acm2 is O linked, although we cannot rule out possible N-glycosylation for two of the peptides.

sWGA lectin blot of surface proteins from *L. plantarum*. The MS analysis of the glycopeptides does not discriminate between HexNAcs with identical masses. Based on the ubiquitous presence of GlcNAc in peptidoglycan and reports of *O*-GlcNAcylation of listerial flagellin and streptococcal serine-rich proteins (37, 52), we hypothesized that Acm2 was modified with GlcNAc. In order to address this question, cell wall-associated proteins were extracted and separated by SDS-PAGE. After transferring the proteins to a blot, they were hybridized with the GlcNAc-specific lectin sWGA. The results (Fig. 3) show a band appearing in the wild-type strain and in the Δ*acm2* strain complemented with a plasmid encoding secreted Acm2 (pAcm2) but not in the non-complemented Δ*acm2* strain. RNase B, which is modified with a GlcNAc-containing glycan, has previously been shown to have WGA reactivity (31) and did indeed show a clear band (Fig. 3A, lane 1). BSA, which is unglycosylated, was utilized as a negative control and indeed did not bind sWGA (Fig. 3A, lane 2). This indicates that Acm2 is glycosylated with GlcNAc. Figure 3 shows that Acm2 migrates slower than expected based on its predicted molecular mass (78.9 kDa), which could be caused by glycosylation. Interestingly, the blots showed strong background signals,

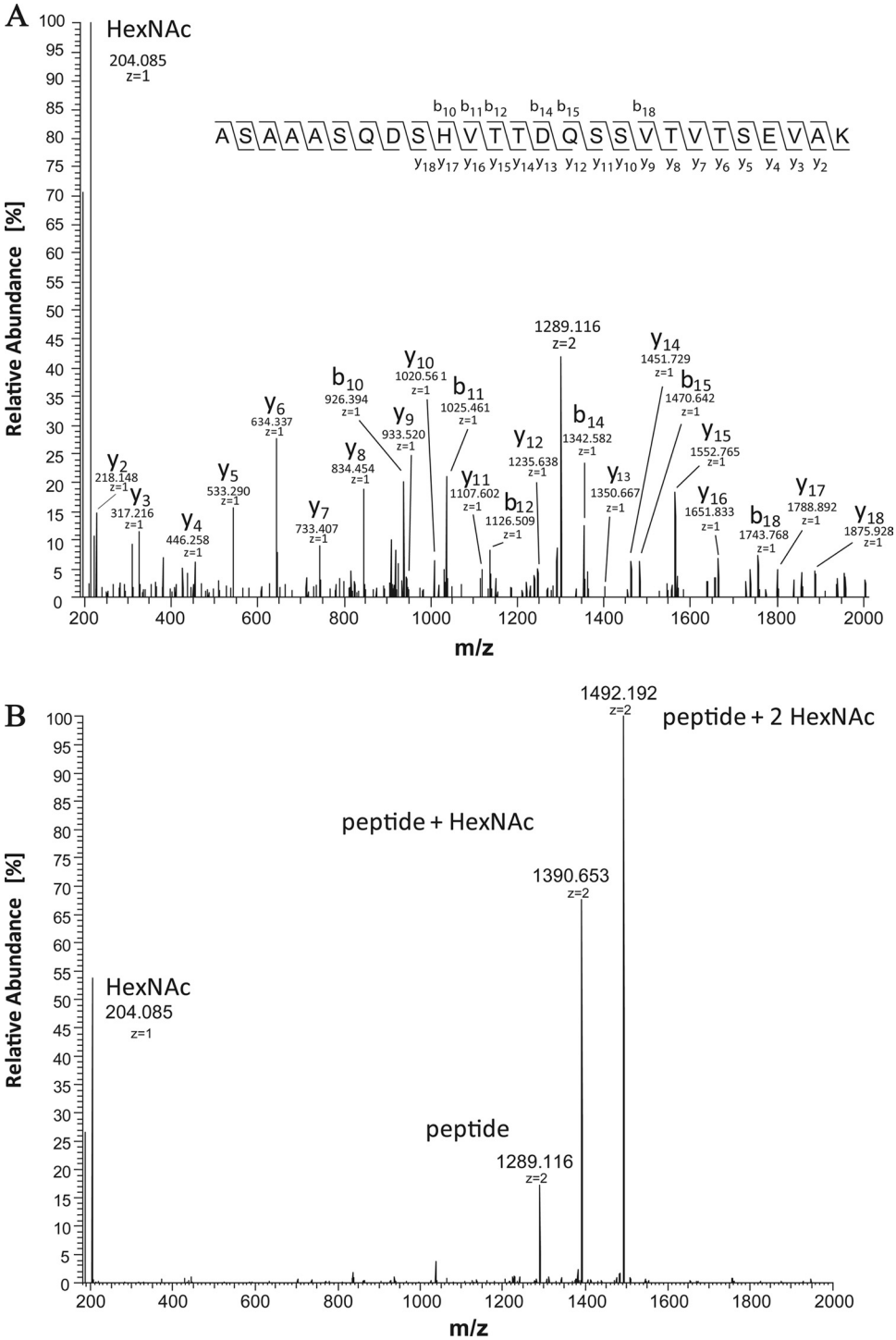

FIG 2 Identification of a representative glycopeptide from Acm2. (A) MS/MS spectrum (collision energy, 50 eV) of a triply charged glycopeptide modified with three HexNAc moieties detected at *m/z* 1,062.829 ($[M + 3H]^{3+}$). The derived mass for the single-charged glycopeptide ($[M+H]^+$) is 3,186.473 Da (theoretical value, 3,186.465 Da). The MS/MS spectrum shows the doubly charged, deglycosylated peptide appearing as a signal at *m/z* 1,289.116 ($[M + 2H]^{2+}$), corresponding to a peptide mass ($[M+H]^+$) of 2,577.225 Da (the theoretical mass is 2,577.227 Da, meaning that the accuracy was better than 1 ppm). The deglycosylation is confirmed by the appearance of the diagnostic ion for HexNAc at *m/z* 204.085 ($[M+H]^+$). Furthermore, the difference between the mass of the precursor ion and the doubly charged full-length ion at *m/z* 1,289.116 ($[M + 2H]^{2+}$) corresponds to 609.248 Da (3,186.473 − 2,577.225), which corresponds to the mass of three HexNAc residues [$(3 \times 204.085) - (3 \times 1.0072) = 609.233$]. The amino acid sequence of the peptide is confirmed by the accurate peptide mass as well as by the detection of fragment y and b ions, as indicated. (B) MS/MS spectrum of the same triply charged glycopeptide at a lower HCD fragmentation energy (35 eV), which led to limited peptide backbone fragmentation but detectable neutral losses of the HexNAc moieties. The diagnostic HexNAc oxonium ion appears as a signal at *m/z* 204.085, and the doubly charged peptide ($[M + 2H]^{2+}$) appears as nonglycosylated, singly glycosylated, and doubly glycosylated fragment ions at *m/z* 1,289.116, 1,390.653 (glycopeptide mass, 2,780.299 Da; $[M+H]^+$), and 1,492.192 (glycopeptide mass, 2,983.377 Da; $[M+H]^+$), respectively.

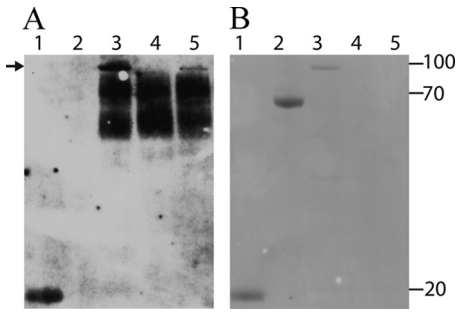

FIG 3 Lectin blot of the surface protein fraction from *L. plantarum*. The cultures were cultivated for 18 h, and the isolated surface proteins were subjected to SDS-PAGE followed by sWGA lectin blotting (A) or staining with Coomassie blue (B). Lanes 1, 1 μg RNase B (positive control); lanes 2, 1 μg BSA (negative control); lanes 3, wild type; lanes 4, Δ*acm2* strain; lanes 5, Δ*acm2* strain transformed with pAcm2. The arrow indicates the Acm2 protein (bands visible in lanes 3 and 5 [A] and lane 3 [B]; note that the amount of Acm2 in lane 5 in panel B is too low to be detectable with Coomassie staining, but the protein is clearly visible in the corresponding lane of the lectin blot [A]). The positions of molecular mass markers (in kDa) are shown on the right.

which may be due to aspecific binding but which also could indicate the presence of additional GlcNAc-containing compounds. Notably, the fact that these proteins are also present in the sample from the Δ*acm2* strain excludes the possibility that these are Acm2 degradation products.

Identification of the subcellular localization of Acm2 glycosylation. To determine the subcellular localization of Acm2 glycosylation, we constructed a strain expressing an intracellular version of the Acm2 protein (Δ*acm2*, pCytAcm2). Initially, we constructed a plasmid encoding Acm2 lacking its predicted signal peptide (32 N-terminal residues, predicted by the SignalP 3.0 Server [3]). We expected this strain to have cell separation defects resulting in cell sedimentation when grown in MRS broth, a phenotype previously observed for *L. plantarum* lacking the *acm2* gene (32). Surprisingly, *L. plantarum* harboring this construct displayed a phenotype similar to that of the wild type, and SDS-PAGE analysis of the surface protein fraction of this strain clearly showed that Acm2 was still secreted (results not shown). In order to determine the glycosylation status of intracellularly expressed Acm2 without the risk of contamination from extracellular Acm2, a second construct, which encoded a variant of Acm2 lacking an additional 79 residues at the N terminus, was made (Fig. 1B). *L. plantarum* harboring this construct displayed a growth phenotype similar to that of the Δ*acm2* knockout strain. Analysis of the surface protein fraction by SDS-PAGE (Fig. 4A) and by our standard and much more sensitive LC-MS/MS method confirmed the absence of extracellular Acm2. The LC-MS/MS analysis (results not shown) did not reveal any Acm2 peptides.

LC-MS/MS analysis of a subfraction of isolated, separated, and in-gel-trypsinized intracellular proteins was then carried out to check the presence and glycosylation status of intracellular Acm2. This analysis revealed the presence of several Acm2-derived peptides, including glycosylated forms of all of the previously detected glycopeptides (two of the five glycopeptides shown in Fig. 1 come from the part of the protein that had been truncated and were therefore not detected). As an example, Fig. 4B shows an MS/MS spectrum for the triple-glycosylated version of the glycopeptide MDSTGPQSQSSASEAAK that includes the N terminus of the truncated Acm2. Note that this peptide, which corresponds to the third peptide shown in Fig. 1C, is the N-terminal peptide of the engineered cytoplasmic Acm2 version (Fig. 1B), explaining why it starts with methionine. The spectrum shows fully and partially deglycosylated full-length fragments of this peptide as well as the signature HexNAc oxonium ion.

DISCUSSION

It was recently suggested that peptidoglycan hydrolases from *L. plantarum* could be glycosylated (20), and glycan modification of AcmB, a peptidoglycan hydrolase from *Lactococcus lactis*, has also been proposed (15). In this study, we demonstrate that the AST domain of the major *L. plantarum* autolysin Acm2 is glycosylated and contains at least 15 sites for HexNAc modification. As is common in the type of LC-MS/MS experiments used for glycopeptide detection, sequence coverage was incomplete (57.1% for the complete protein, 83.2% for the AST domain), so it is possible that additional glycosylation sites exist. The blotting experiments indicate that the HexNAc moieties attached to Acm2 are GlcNAcs. Studies with a truncated version of Acm2 indicated that GlcNAc modification of Acm2 is an intracellular process.

Interestingly, the nature of Acm2 glycosylation is similar to protein glycosylation found in Gram-positive pathogens, in particular for flagellin from *Listeria monocytogenes* (37) and the serine-rich adhesins from streptococci (52). It has been shown that O-glycosylation of both the listerial flagellin and the large surface adhesin GspB from *Streptococcus gordonii* with GlcNAc most likely occurs in the cytoplasm (39, 46).

The conclusion that glycosylation of Acm2 is an intracellular process was drawn from experiments with an N-terminally truncated version of the protein that was no longer secreted. Surprisingly, Acm2 was still secreted after removal of its predicted signal peptide (32 residues, predicted by SignalP; http://www.cbs.dtu.dk/services/SignalP). Interestingly, SignalP predicted an alternative SPase I processing site located between residues 68 and 69, which may explain why the Acm2 variant lacking the 32-residue signal peptide was still secreted. Therefore, an Acm2 variant lacking the 111 N-terminal residues and free of SPase I processing sites according to SignalP was constructed (Fig. 1B). It remains to be determined whether the N-terminal part of the AST domain that had to be removed to create intracellular Acm2 is somehow involved in secretion under natural conditions.

Acm2 glycopeptides were typically detected in several glycosylation states (Fig. 1C), suggesting that the glycosylation of Acm2 could be of a dynamic nature. Recently, Børud and colleagues reached similar conclusions in their studies on glycosylation of neisserial pilin (7). Since O-glycosylation by GlcNAc is an important dynamic regulatory signal in eukaryotic cells (51), one may speculate that the glycosylation of Acm2 has a regulatory function.

One intriguing and important question is which glycosyltransferase(s) is responsible for the modification detected in this study. Glycosyltransferases involved in GlcNAc modification of listerial flagellin (GmaR) and the streptococcal Fap1 adhesin (Gtf1) have been identified (8, 39, 49). The *L. plantarum* genome contains six genes that encode putative glycosyltransferases (TagE1 to TagE6) that share sequence similarities with Gtf1 (>20% sequence identity), making it tempting to speculate that the glycosyltransferase responsible for Acm2 glycosylation is among these enzymes. Searches for homologues of known bacterial O-GlcNAcases (9, 38) did not yield any candidate genes putatively encoding enzymes that could be responsible for deglycosylation of Acm2. Clearly,

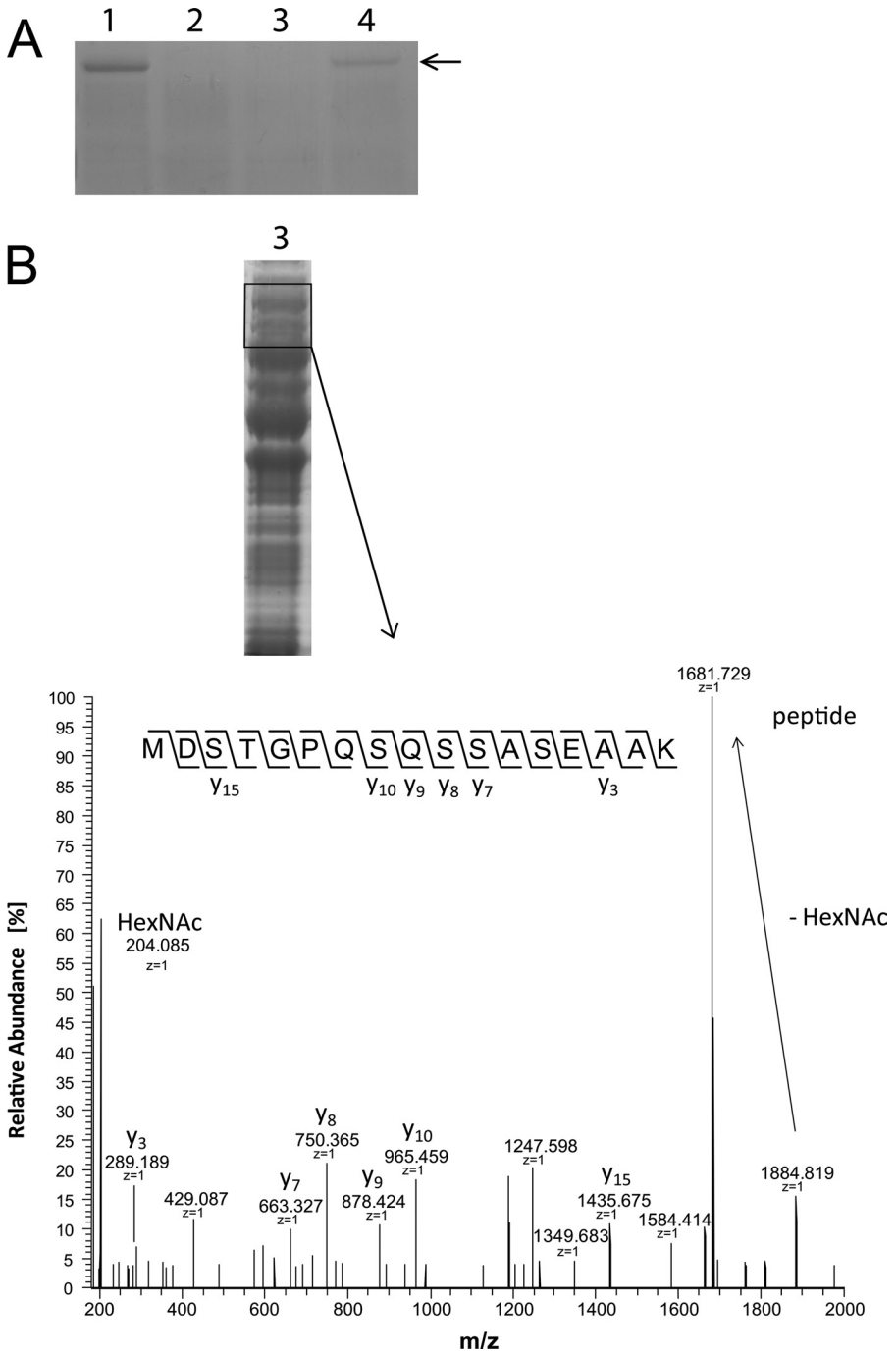

FIG 4 Glycosylation analysis of a peptide obtained from intracellular Acm2. Surface proteins and proteins from lysed cells were separated by SDS-PAGE. (A) Coomassie-stained SDS-PAGE gel of the surface protein fraction isolated from *L. plantarum*. Lane 1, wild type; lane 2, Δ*acm2* strain; lane 3, Δ*acm2* strain complemented with pCytAcm2; lane 4, Δ*acm2* strain complemented with pAcm2. Acm2 is indicated by the arrow. (B) Intracellular proteins from sample 3 (Δ*acm2* strain complemented with pCytAcm2) were separated by SDS-PAGE, and a subfraction (boxed) was in-gel trypsinized and analyzed by mass spectrometry. The MS/MS spectrum (collision energy, 35 eV) of the doubly charged glycopeptide MDSTGPQSQSSASEAAK modified with three HexNAcs is shown (*m/z* 1,145.992; calculated mass for $[M+H]^+$, 2,290.977 Da; theoretical mass for $[M+H]^+$, 2,290.971 Da). A fragment corresponding to the peptide modified with one HexNAc is shown at *m/z* 1,884.819 ($[M+H]^+$), and the naked peptide backbone gives an ion with *m/z* 1,681.729 ($[M+H]^+$). The spectrum is dominated by the glycan oxonium ion ($[M+H]^+$) at *m/z* 204.085. The identity of the peptide is confirmed by the accurate peptide mass (theoretical mass for the nonglycosylated peptide, $[M+H]^+$, = 1,681.733 Da; accuracy, 2 ppm) as well as the detection of minor amounts of fragment ions, as indicated.

more work is needed to identify the enzymes involved in Acm2 glycosylation and to create a deeper understanding of the functional implications of protein glycosylation in lactobacilli. One related question concerns the possibility that other *Lactobacillus* proteins are also glycosylated. For example, the N-terminal AST domain of Acm2 is found in an additional 10 of the 16 peptidoglycan hydrolases in *L. plantarum* (20), and some of these might be glycosylated.

The characterization of glycoproteins in probiotic lactobacilli is still in its infancy, and it is likely that more knowledge of such glycoproteins will contribute to our understanding of the surface biology, colonization ability, and symbiotic host interactions of these bacteria.

ACKNOWLEDGMENTS

We thank Iris van Swam for excellent technical guidance during the construction of the Acm2 knockout mutant.

This work was supported by Norwegian Research Council grants 159058, 183627, 183637, and 186032 and by funds from GlycoNor, the Department of Molecular Biosciences, and the Center for Molecular Biology and Neurosciences of the University of Oslo.

REFERENCES

1. **Ahrne S, et al.** 1998. The normal Lactobacillus flora of healthy human rectal and oral mucosa. J. Appl. Microbiol. **85**:88–94.
2. **Banerjee A, Ghosh SK.** 2003. The role of pilin glycan in neisserial pathogenesis. Mol. Cell. Biochem. **253**:179–190.
3. **Bendtsen JD, Nielsen H, von Heijne G, Brunak S.** 2004. Improved prediction of signal peptides: SignalP 3.0. J. Mol. Biol. **340**:783–795.
4. **Bensing BA, Gibson BW, Sullam PM.** 2004. The *Streptococcus gordonii* platelet binding protein GspB undergoes glycosylation independently of export. J. Bacteriol. **186**:638–645.
5. **Bernard E, et al.** 2011. Characterization of O-acetylation of *N*-acetylglucosamine: a novel structural variation of bacterial peptidoglycan. J. Biol. Chem. **286**:23950–23958.
6. **Boekhorst J, Wels M, Kleerebezem M, Siezen RJ.** 2006. The predicted secretome of *Lactobacillus plantarum* WCFS1 sheds light on interactions with its environment. Microbiology **152**:3175–3183.
7. **Børud B, et al.** 2010. Genetic, structural, and antigenic analyses of glycan diversity in the O-linked protein glycosylation systems of human *Neisseria* species. J. Bacteriol. **192**:2816–2829.
8. **Bu S, et al.** 2008. Interaction between two putative glycosyltransferases is required for glycosylation of a serine-rich streptococcal adhesin. J. Bacteriol. **190**:1256–1266.
9. **Dennis RJ, et al.** 2006. Structure and mechanism of a bacterial β-glucosaminidase having O-GlcNAcase activity. Nat. Struct. Mol. Biol. **13**:365–371.
10. **de Vries MC, Vaughan EE, Kleerebezem M, de Vos WM.** 2006. *Lactobacillus plantarum*—survival, functional and potential probiotic properties in the human intestinal tract. Int. Dairy J. **16**:1018–1028.
11. **Dobos KM, Khoo KH, Swiderek KM, Brennan PJ, Belisle JT.** 1996. Definition of the full extent of glycosylation of the 45-kilodalton glycoprotein of *Mycobacterium tuberculosis.* J. Bacteriol. **178**:2498–2506.
12. **Fletcher CM, Coyne MJ, Villa OF, Chatzidaki-Livanis M, Comstock LE.** 2009. A general O-glycosylation system important to the physiology of a major human intestinal symbiont. Cell **137**:321–331.
13. **Fredriksen L, Mathiesen G, Sioud M, Eijsink VG.** 2010. Cell wall anchoring of the 37-kilodalton oncofetal antigen by *Lactobacillus plantarum* for mucosal cancer vaccine delivery. Appl. Environ. Microbiol. **76**: 7359–7362.
14. **Horton RM, Cai ZL, Ho SN, Pease LR.** 1990. Gene splicing by overlap extension: tailor-made genes using the polymerase chain reaction. Biotechniques **8**:528–535.
15. **Huard C, et al.** 2003. Characterization of AcmB, an *N*-acetylglucosaminidase autolysin from *Lactococcus lactis.* Microbiology **149**: 695–705.
16. **Josson K, et al.** 1989. Characterization of a gram-positive broad-host-range plasmid isolated from *Lactobacillus hilgardii.* Plasmid **21**:9–20.
17. **Karlyshev AV, et al.** 2004. The *Campylobacter jejuni* general glycosylation system is important for attachment to human epithelial cells and in the colonization of chicks. Microbiology **150**:1957–1964.
18. **Killmann H, Herrmann C, Torun A, Jung G, Braun V.** 2002. TonB of *Escherichia coli* activates FhuA through interaction with the β-barrel. Microbiology **148**:3497–3509.
19. **Kleerebezem M, et al.** 2003. Complete genome sequence of *Lactobacillus plantarum* WCFS1. Proc. Natl. Acad. Sci. U. S. A. **100**:1990–1995.
20. **Kleerebezem M, et al.** 2010. The extracellular biology of the lactobacilli. FEMS Microbiol. Rev. **34**:199–230.
21. **Lambert JM, Bongers RS, Kleerebezem M.** 2007. Cre-*lox*-based system for multiple gene deletions and selectable-marker removal in *Lactobacillus plantarum.* Appl. Environ. Microbiol. **73**:1126–1135.
22. **Lazar IM, Lazar AC, Cortes DF, Kabulski JL.** 2011. Recent advances in the MS analysis of glycoproteins: theoretical considerations. Electrophoresis **32**:3–13.
23. **Logan SM.** 2006. Flagellar glycosylation—a new component of the motility repertoire? Microbiology **152**:1249–1262.
24. **Lu JZ, Fujiwara T, Komatsuzawa H, Sugai M, Sakon J.** 2006. Cell wall-targeting domain of glycylglycine endopeptidase distinguishes among peptidoglycan cross-bridges. J. Biol. Chem. **281**:549–558.
25. **Mathiesen G, et al.** 2004. High-level gene expression in *Lactobacillus plantarum* using a pheromone-regulated bacteriocin promoter. Lett. Appl. Microbiol. **39**:137–143.
26. **Mathiesen G, Sveen A, Piard JC, Axelsson L, Eijsink VG.** 2008. Heterologous protein secretion by *Lactobacillus plantarum* using homologous signal peptides. J. Appl. Microbiol. **105**:215–226.
27. **Mobili P, et al.** 2009. Heterogeneity of S-layer proteins from aggregating and non-aggregating Lactobacillus kefir strains. Antonie Von Leeuwenhoek **95**:363–372.
28. **Molin, G.** 2001. Probiotics in foods not containing milk or milk constituents, with special reference to *Lactobacillus plantarum* 299v. Am. J. Clin. Nutr. **73**:380S–385S.
29. **Möschl A, et al.** 1993. Characterization of the S-layer glycoproteins of two lactobacilli, p. 281–284. *In* Beveridge TJ, Koval SF (ed.), Advances in bacterial paracrystalline surface layers. Plenum, New York, NY.
30. **Nothaft H, Szymanski CM.** 2010. Protein glycosylation in bacteria: sweeter than ever. Nat. Rev. Microbiol. **8**:765–778.
31. **Oguri S.** 2005. Analysis of sugar chain-binding specificity of tomato lectin using lectin blot: recognition of high mannose-type N-glycans produced by plants and yeast. Glycoconj. J. **22**:453–461.
32. **Palumbo E, et al.** 2006. D-Alanyl ester depletion of teichoic acids in *Lactobacillus plantarum* results in a major modification of lipoteichoic acid composition and cell wall perforations at the septum mediated by the Acm2 autolysin. J. Bacteriol. **188**:3709–3715.
33. **Plummer C, et al.** 2005. A serine-rich glycoprotein of *Streptococcus sanguis* mediates adhesion to platelets via GPIb. Br. J. Haematol. **129**: 101–109.
34. **Remus DM, Kleerebezem M, Bron PA.** 2011. An intimate tête-à-tête—how probiotic lactobacilli communicate with the host. Eur. J. Pharmacol. **668**(Supp. 1):S33–S42.
35. **Ritchie MA, Gill AC, Deery MJ, Lilley K.** 2002. Precursor ion scanning for detection and structural characterization of heterogeneous glycopeptide mixtures. J. Am. Soc. Mass Spectrom. **13**:1065–1077.
36. **Schaffer, C, and Messner P.** 2004. Surface-layer glycoproteins: an example for the diversity of bacterial glycosylation with promising impacts on nanobiotechnology. Glycobiology **14**:31R–42R.
37. **Schirm M, et al.** 2004. Flagellin from *Listeria monocytogenes* is glycosylated with β-O-linked *N*-acetylglucosamine. J. Bacteriol. **186**:6721–6727.
38. **Sheldon WL, et al.** 2006. Functional analysis of a group A streptococcal glycoside hydrolase Spy1600 from family 84 reveals it is a β-*N*-acetylglucosaminidase and not a hyaluronidase. Biochem. J. **399**:241–247.
39. **Shen A, Kamp HD, Grundling A, Higgins DE.** 2006. A bifunctional O-GlcNAc transferase governs flagellar motility through anti-repression. Genes Dev. **20**:3283–3295.
40. **Shevchenko A, Tomas H, Havlis J, Olsen JV, Mann M.** 2006. In-gel digestion for mass spectrometric characterization of proteins and proteomes. Nat. Protoc. **1**:2856–2860.
41. **Siboo IR, Chaffin DO, Rubens CE, Sullam PM.** 2008. Characterization of the accessory Sec system of *Staphylococcus aureus.* J. Bacteriol. **190**: 6188–6196.
42. **Siezen RJ, et al.** 2010. Phenotypic and genomic diversity of *Lactobacillus plantarum* strains isolated from various environmental niches. Environ. Microbiol. **12**:758–773.
43. **Sørvig E, et al.** 2003. Construction of vectors for inducible gene expression in *Lactobacillus sakei* and *L plantarum.* FEMS Microbiol. Lett. **229**: 119–126.
44. **Stepper J, et al.** 2011. Cysteine S-glycosylation, a new post-translational modification found in glycopeptide bacteriocins. FEBS Lett. **585**:645–650.
45. **Szymanski CM, Wren BW.** 2005. Protein glycosylation in bacterial mucosal pathogens. Nat. Rev. Microbiol. **3**:225–237.
46. **Takamatsu D, Bensing BA, Sullam PM.** 2004. Four proteins encoded in the gspB-secY2A2 operon of *Streptococcus gordonii* mediate the intracel-

lular glycosylation of the platelet-binding protein GspB. J. Bacteriol. **186**: 7100–7111.
47. **van Baarlen P, et al.** 2009. Differential NF-κB pathways induction by *Lactobacillus plantarum* in the duodenum of healthy humans correlating with immune tolerance. Proc. Natl. Acad. Sci. U. S. A. **106**:2371–2376.
48. **Vik A, et al.** 2009. Broad spectrum O-linked protein glycosylation in the human pathogen *Neisseria gonorrhoeae.* Proc. Natl. Acad. Sci. U. S. A. **106**:4447–4452.
49. **Wu R, Wu H.** 2011. A molecular chaperone mediates a two-protein enzymatic complex and glycosylation of serine-rich streptococcal adhesins. J. Biol. Chem. **286**:34923–34931.
50. **Xu Q, et al.** 2009. Structural basis of murein peptide specificity of a gamma-D-glutamyl-L-diamino acid endopeptidase. Structure **17**: 303–313.
51. **Zachara NE, Hart GW.** 2006. Cell signaling, the essential role of O-GlcNAc! Biochim. Biophys. Acta **1761**:599–617.
52. **Zhou M, Wu H.** 2009. Glycosylation and biogenesis of a family of serine-rich bacterial adhesins. Microbiology **155**:317–327.